

A Computational Intelligence based MPPT for PV Power Generation System with Small-Signal Analysis

Manoj Kumar Senapati¹, C. R. Pradhan^{2*,†}, and Rajnish Kaur Calay³

¹*Department of Electrical Engineering, Indian Institute of Technology (ISM) Dhanbad, India*

²*Department of Electrical Engineering, The Arctic University of Norway, Narvik Campus, Norway*

³*Department of Building, Energy and Material Technology, UiT The Arctic University of Norway,*

SUMMARY

The perturb and observe (P&O) may fail to track the global maximum power point (GMPP) under partial shading conditions (PSCs) due to the existence of multiple peak functions in its output power characteristic curve of a photovoltaic (PV) array. Therefore, a reliable maximum power point tracking (MPPT) technique is essential to track the global maximum power point (GMPP) within an appropriate time. This paper proposes a hybrid MPPT technique by combining an evolutionary optimization technique namely the modified invasive weed optimization (MIWO) with the conventional P&O algorithm to enhance the search performance. MIWO executes in the initial stages of the tracking followed by the P&O at the final stages in the MPPT search process. The combined approach ensures faster convergence and better search to the GMPP under rapid climate change and PSCs. The search performance of the hybrid MIWO-P&O technique is examined on a standalone PV system through both MATLAB/Simulink environment and experimentally using dSPACE (DS1103)-based real-time microcontroller hardware set up. The performance of the proposed hybrid MPPT scheme is compared with the recent state-of-the-art MPPPT techniques. In addition, the small-signal analysis of the PV system is carried out to evaluate the loop robustness of the controller design. For a given set of system parameters, simulations for the small-signal model and robustness studies are analyzed to verify the results. The overall results justify the efficacy of the proposed hybrid MPPT algorithm.

KEYWORDS: Maximum power point tracking, modified invasive weed optimization, perturb and observe, photovoltaic, small-signal analysis.

*Correspondence to: Chittaranjan Pradhan, *Department of Electrical Engineering, UiT The Arctic University of Norway, Norway*

†E-mail: chittaranjan.pradhan@uit.no

1. INTRODUCTION

In the past few decades, electricity generation has been increasing significantly using renewable energy resources (RESs) across the globe due to the rapid depletion of fossil fuels, increased oil prices and global warming [1]. Among the various RESs, solar photovoltaic (PV) power is one of the most popular source owing to numerous advantages such as it is omnipresent, freely available, absence of rotating parts, low operational cost, almost maintenance-free, accommodation in rooftops, environment-friendly etc, [2]. However, there are several technical and non-technical challenges observed in PV power generation such as low power conversion efficiency, high installation cost, and high dependency on atmospheric conditions, etc. [3].

In a PV power generation system, the maximum power point (MPP) is a unique point in the power–voltage (P – V) characteristics curve at given solar insolation/irradiation and ambient temperature and it varies with environmental conditions. To track the nonlinear nature of the P – V curve and ensure that the highest possible power is extracted from the PV array, a maximum power point tracking (MPPT) technique is an integral part of the PV system [3]. To accomplish the optimal performance under uniform and nonuniform irradiances and partial shading conditions (PSCs), various MPPT techniques have emerged in the last few decades to extract the maximum power and some of them are being installed in the PV power generation system successfully. Efficacy of an MPPT controller is decided based on its hardware and software implementation complexity, robustness, the requirement of several sensors, convergence speed, etc. [7-8].

The available MPPT techniques are broadly categorized into conventional methods [4]-[9], artificial intelligence methods [10]-[12] and bio-inspired methods [13]-[27]. The P&O, hill-climbing, incremental conductance, short-circuit current and open-circuit voltage techniques are the most popular of conventional methods to MPP tracking [10]. However, In PSCs, where there are multiple MPPs in the P – V curve, the conventional algorithms may fail in attaining the global MPP (GMPP) among the local MPPs, consequently decreasing the overall efficiency of the PV system [3-6]. Concerning the multiple-peak issue during PSCs, numerous solutions have been projected by modifying the conventional algorithms.

Meanwhile, the artificial intelligence techniques such as fuzzy logic controller (FLC) [4] and artificial neural network (ANN) [13] are suggested in the previous literature. In [9], a modified incremental algorithm has been used to track the GMPP under different types of partial shading conditions and load variations. To improve the MPPT capability of single algorithm further, several hybrid intelligent methods such as fuzzy based modified hill climbing [11], fuzzy based ant colony optimization [12], fuzzy logic based

variable step incremental conductance method [16], neuro-fuzzy based [17] and genetic algorithm (GA)-fuzzy logic are also reported in the literature. These approaches give satisfactory results for tracking the GMPP under PSCs. However, the FLC-based MPPT schemes require the knowledge base to create rules for tracking and hence, need a large memory size. On the other hand, the ANN-based MPPT schemes require huge data for training and hence, involve complex computation and storage. To alleviate these problems further, several bio-inspired-based MPPT techniques have been proposed in the literature.

The optimal searching ability without involving excessive mathematical computations [19], handling of complex nonlinearity and implementation simplicity make these bio-inspired algorithms more attractive for solving the MPPT problems, especially under PSCs. The Particle swarm optimization (PSO) [20], Ant colony optimization (ACO) [21], Fusion firefly algorithm [22], Hybrid BAT-fuzzy controller based MPPT [23], Simulated annealing (SA) [24], Flower pollination (FPA) [25], Jaya optimization [26], modified butterfly optimization algorithm (MBOA) [27], etc, come under bio-inspired algorithms. The MBOA MPPT technique has improved MPPT search performance than PSO, differential evolution (DE) and grey wolf optimization (GWO) techniques under partial shading patterns, uniform shading, and load variation conditions [27]. Several hybrid MPPT methods are also reported by combining two or more algorithms together for further improvement in the above-mentioned single algorithms. These are GWO-FLC [28], Particle swarm optimization with perturb & observe (PSO-P&O) [29], Jaya with differential evolutionary algorithm (Jaya-DE) [30], the combination of the DE algorithm with particle swarm optimization (DEPSO) [31] are such few examples. The overall search performances of hybrid computational intelligence algorithms are superior to a single computational intelligence technique. However, speed of response, controller design complexity, and implementation of hardware cost of hybrid MPPT algorithm is still challenging.

The aforementioned study clearly shows that a significant number of research articles are dedicated to solving the MPPT problem especially during PSCs and rapid weather change conditions. However, very few reported methods could give a satisfactory solution for every possible operating condition. This motivates us to develop a new algorithm that can be computationally efficient and have fast convergence to GMPP even under extreme weather conditions. In this paper, a new hybrid MPPT technique is proposed where the salient features of modified invasive weed optimization (MIWO) are suitably integrated with the traditional P&O algorithm. IWO is inspired from colonizing weeds and has better robustness, adaptation, and randomness like colonizing weeds [32]. IWO is a population-based search technique and is widely used in solving many engineering problems [32]. The main advantage of IWO is that it can produce new weeds from all weeds. The weeds having the best fitness value can produce a greater number of weeds. Similarly, weeds

having the worst fitness value can produce a smaller number of weeds around their parent weeds. This property improves the convergence of IWO. Further, the new weeds are distributed normally over the search space. Normal distribution generates random numbers without mating, so any two of the weeds cannot occupy the same position. Due to this property, IWO explores the whole search space.

Due to the above-mentioned features of IWO, it can effectively search the GMPP of a PV system under PSCs and extreme weather changing conditions. Hence, combining IWO with conventional P&O can significantly enhance the MPPT performance of PV system.

The main features of this research work are summarized as follows:

- A hybrid MIWO-P&O computational technique is introduced to track the GMPP of the PV system under PSCs.
- The efficacy of the proposed control technique is validated by comparing it with two existing MPPT techniques [27, 28].
- The small-signal analysis of the PV system is carried out to analyse loop robustness of the controller design with the variation of loads.
- Both simulation as well as experimental results are presented to verify the search performance of the hybrid MIWO-P&O technique under PSCs and variation of load.

The rest of the paper is organised as follows. The modeling of the PV system and the effect of partial shading on the performance of the PV module is discussed in Section-2. A detail description of the proposed MIWO-P&O-based hybrid MPPT technique is provided in Section-3. Simulation and experimental results are provided in Section-4 and Section-5, respectively. The small-signal analysis of the proposed PV system is carried out in Section-6. In Section-7, the performance of the proposed algorithm is compared with the state-of-the-art techniques. Finally, the paper is concluded in Section 8.

2. PV SYSTEM

In the present work, the standalone PV system as shown in Fig. 1 is considered for performance evaluation of the proposed hybrid MIWO-P&O MPPT algorithm. As shown in the figure, the PV system is supplying power to a DC load through a boost converter. The switching of the boost converter is controlled by the proposed MIWO-P&O algorithm.

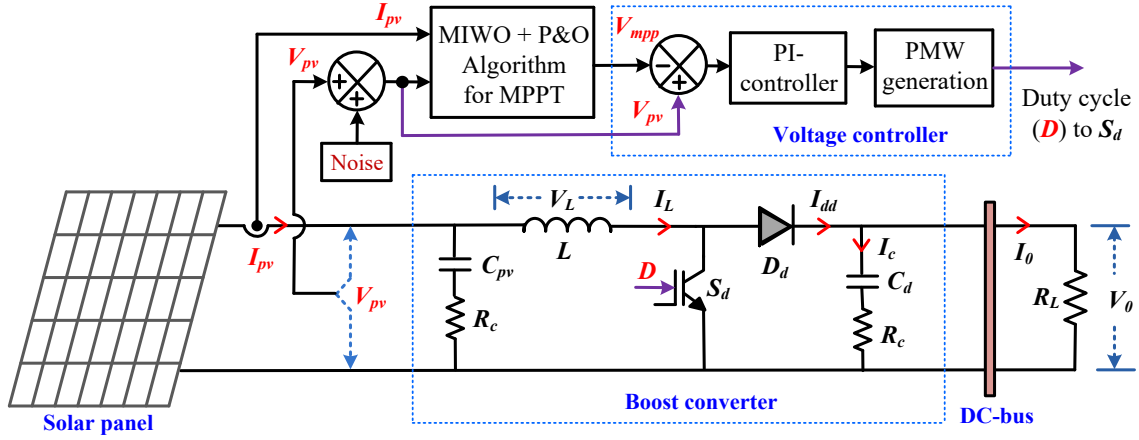


Figure 1. PV system with boost converter for MPPT

The PV system with shading pattern is simulated in MATLAB [33]. A PV module can be considered a voltage-controlled current source connected in parallel with a diode [34]. The equivalent circuit of the PV cell is shown in Fig. 2. The PV array is described by current-voltage characteristic function [33] as:

$$I_{PV} = n_p I_{ph} - I_{rs} \left[\exp \left(\frac{q(V_{pv} + I_{pv} R_s)}{AKTn_s} \right) - 1 \right] - \frac{V_{pv} + I_{pv} R_s}{R_{sh}} \quad (1)$$

where, n_s and n_p are the number of cells connected in series and in parallel, $q=1.602 \times 10^{-19} \text{C}$ is the electron charge, $K=1.3806 \cdot 10^{-23} \text{ J/K}$ is Boltzman's constant, $A=2$ is the P-N junction's ideality factor, T is the cell's temperature (K), I_{ph} is the cell's photocurrent which depends on the solar irradiation and temperature, I_{rs} is the cell's reverse saturation current, V_{pv} is cell voltage.

$$I_{ph} = I_{sc} \frac{G}{G^*} \quad (2)$$

where, G is the solar irradiance, I_{sc} is the short circuit current at standard test condition and G^* is reference solar irradiance (i.e. 1000 w/m^2).

$$I_{Dp} = I_{rs} \left[\exp \left(\frac{q(V_{pv} + I_{pv} R_s)}{AKTn_s} \right) - 1 \right] \quad (3)$$

Where, I_{Dp} represents the current flowing through the diode in Fig. 2.

According to P - V characteristics of PV system, PV can generate maximum power at a particular voltage which is called as the voltage at maximum power point (V_{mpp}). The P - V characteristics with different levels of irradiance are shown in Fig. 2 under consideration of non-uniform irradiance. In this study, the PV system consists of one parallel string and each string is asserted with 4 series connected modules. Each module has power rating of 280W. The PV string during partial shading conditions with different irradiance level are simulated as given in Fig.3 as specified in Table-1.

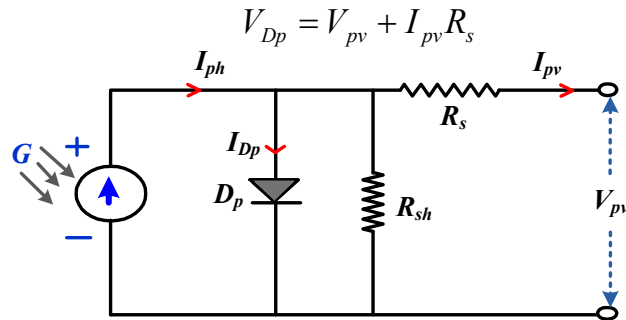


Figure 2: Equivalent diagram of PV cell

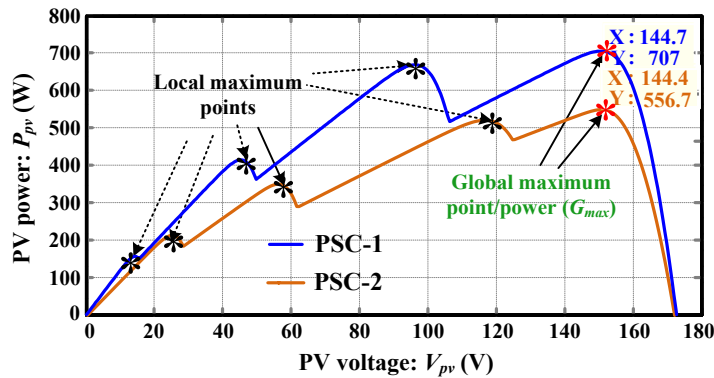


Figure 3. P-V characteristics during partial shading condition

Table 1: Partial shading patterns of PV string

Pattern	For one PV string
1	[Partial shading condition-1] Modules: 1=1000W/m ² , modules: 2=900W/m ² , modules: 3=600W/m ² , modules: 4=300W/m ²
2	[Partial shaded condition-2] Modules: 1=800W/m ² , modules: 2=600W/m ² , modules: 3=500W/m ² , modules: 4=350W/m ²

3. MIWO+P&O MPPT ALGORITHM

A) P&O algorithm

The P&O algorithm has the advantage of simple software and hardware realization [33]. In this implementation, the reference voltage (V_{mpp}) is perturbed in an arbitrary direction and the power levels of two consecutive samples are compared. Depending upon the sign of the power change, the direction for further perturbation is decided. A feedback control loop ensures that the output voltage tracks its reference. The following equation is followed to locate the voltage at which the MPP is reached [35].

$$V_{mpp}(k) = V_{mpp}(k-1) + \Delta V \times \text{sign}\left(\frac{dP_{pv}}{dV_{pv}}\right) \quad (4)$$

where, ΔV and k are the step voltage and iteration, respectively.

However, the conventional P&O algorithm fails to track proper V_{mpp} point under partial shaded condition because of many local maximum power points as shown in Fig. 4. Therefore, the MIWO technique is integrated to P&O algorithm to track the global maximum point in all the available maximum power points. With respect to the DC–DC converter topology, the boost converter, which is also known as the step-up converter, is considered as the most advantageous in this application because of its simplicity, low cost, and high efficiency [34]. Hence, in this paper, a boost converter is considered for MPPT converter as shown in Fig. 1. A modified IWO (MIWO) algorithm was implemented for the effective operation of system under various conditions.

B) MIWO algorithm

Invasive weed optimization is a population based stochastic optimization technique that is grounded on the behaviour of colonization of weeds [32]. It has been attracting the researcher's attention for a decade. Due to its outstanding characteristics like reproduction, spatial dispersal, and competitive exclusion, compared to other the state-of-the-art evolutionary algorithms, it has been utilized in many applications of Engineering and Sciences. Basically, the following steps are involved in MIWO [32]:

Step-1: Initialization: A finite number of a population is generated randomly over the search space within the variable's scope.

Step-2: Reproduction: After getting into a blooming tree, each candidate weed of the population is allowed to produce new weeds and the number of new weeds of a candidate weed depends on its relative the best and the worst fitness value. It is linearly decreased from an allowable maximum weed (S_{max}) to minimum weeds (S_{min}) with S_{max} for the best candidate weed, S_{min} for the worst candidate weed in the population.

$$n(w_i) = \frac{S_{\max}(fit_{\max} - fit(w_i)) + S_{\min}(fit(w_i) - fit_{\min})}{fit_{\max} - fit_{\min}} \quad (5)$$

where, $n(w_i)$ is the number of producing seeds of i^{th} weed, S_{\max} and S_{\min} are predefined parameters. $fit(w_i)$ is the fitness value of i^{th} weed, fit_{\max} and fit_{\min} are maximum and minimum fitness values of the population, respectively.

Step-3: Spatial dispersal: The newly generated weeds are normally distributed over the search space with mean of parent weed position and the varying standard deviation, defined as

$$\sigma_{gen} = \frac{(gen_{\max} - gen)^{mi}}{gen_{\max}^{mi}} (\sigma_{\max} - \sigma_{\min}) + \sigma_{\min} \quad (6)$$

where, σ_{gen} is the standard deviation (SD) at the present generation, σ_{\max} and σ_{\min} are the maximum and minimum standard deviations, predefined parameters, gen_{\max} is the maximum generations, mi is the nonlinear modulation index and necessity of mi is generated seeds could be close to the parent weed.

Step-4: Competitive Exclusion: If a plant leaves no offspring, then it would go extinct, otherwise it would take over the world. Sources will be for some weeds in the field, as there is a competition between weeds to limit the number of weeds in the population. If the sum of parent weeds and the new generated weeds exceeds the maximum limit (W_{\max}), the weeds having worst fitness value are removed up to W_{\max} from the population.

Step-5: Termination Condition:

- (1). The present iteration is equal to the upper limit of the number of iterations
- (2). The above process (Steps 1-4) has been reached the maximum number of fitness evaluations
- (3). $|f(x^*) - f(x)| \leq \varepsilon$ where x^* is the best optimal solution, x is the best solution obtained and ε is a small tolerance value, is defined by the user. If the process (Steps 1-4) meets any one of the aforementioned conditions, it will be terminated.

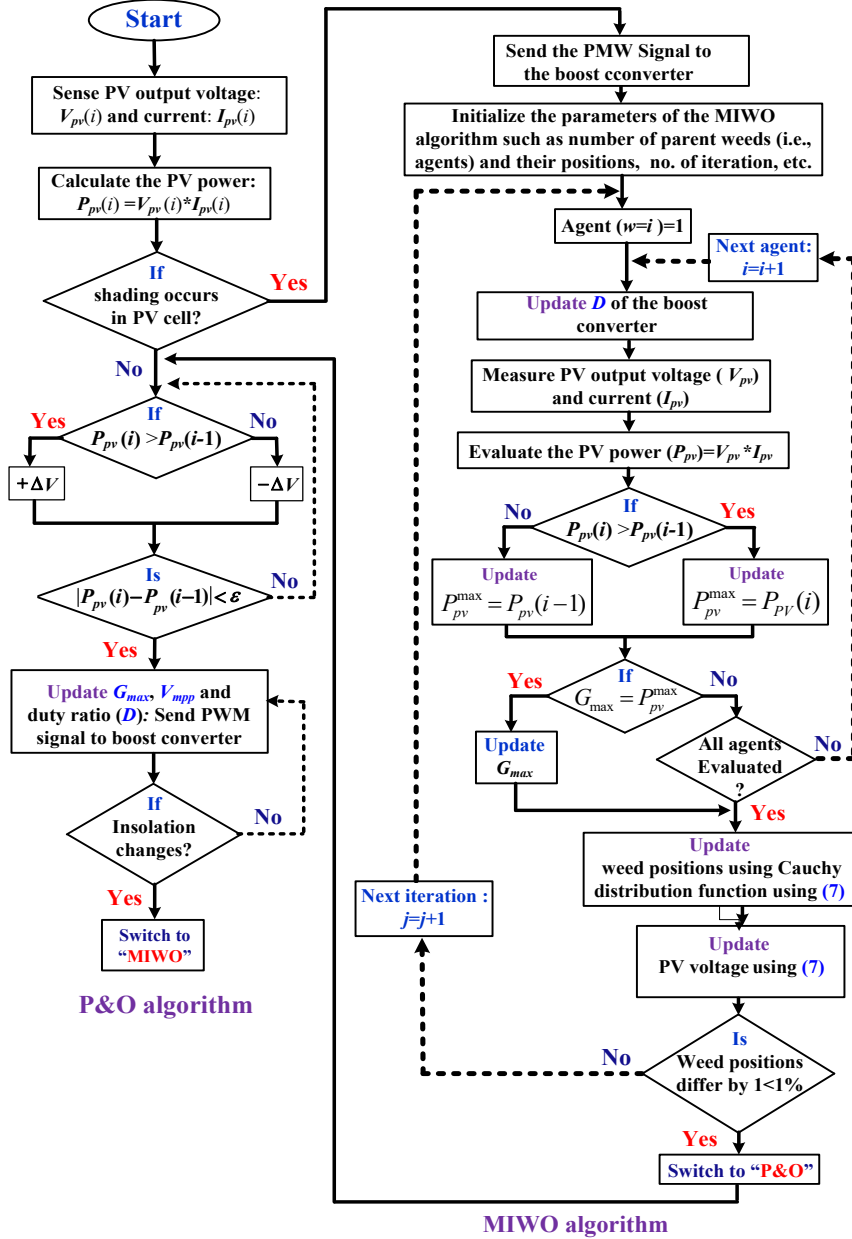


Figure 4. Flowchart of the proposed MPPT algorithm

Generally, the Gaussian function is used in IWO algorithm. For the IWO algorithm reproduction mode, it can generate offspring based on the parent individual super posited Gauss distribution of random variables. To find the optimal reproductive performance, the Cauchy distribution function can give better results instead of Gauss distribution [32, 36]. The Cauchy distribution is smaller than Gauss distribution in the vertical direction. Moreover, in the horizontal direction, Cauchy distribution has become wider when it is near the horizontal axis. Therefore, the Gaussian distribution function has a greater probability to generate small perturbations, but not very large disturbances [32]. But the

Cauchy distribution function has small perturbations capacity than Gauss function, but it is stronger than the Gauss in large distribution. It is expected to have a higher probability of escaping from a local optimum or moving away from a plateau, especially when the “basin of attraction” of the local optimum or the plateau is large relative to the mean steep size [36]. Therefore, the character of the Cauchy distribution can better maintain the population diversity and make the algorithm a better global optimization algorithm and reliability. Hence, the Cauchy distribution function can get a rapidly, optimal solution [34, 36]. Therefore, the Cauchy distribution function is used in IWO algorithm instead of Gaussian distribution function and it is called as modified IWO (MIWO) algorithm. Generally, weather conditions will rapidly change, hence, in this paper implemented MIWO algorithm.

In MIWO, W_{max} seeds are generated around the parent seed. The same principle is applied here and generated W_{max} voltage points around the previous voltage value. Further, P&O algorithm is also included to generate the new value of voltage. Hence, new calculated PV power found from number can get from W_{max} number of voltages. So, the W_{max} number of power points can be calculated to finally optimized P_{pv}^{max} . This process will be continued up to the completion of search space. The new value of voltage can be obtained by

$$V_i^{j+1} = V_i^j + m\sigma_{iter} \times Cauchy(0,1) \times (V_{best} - V_i^j); \quad i=1, 2, \dots, W_{max} \quad (7)$$

where, V_i^j is the i^{th} weed position at j^{th} iteration. V_i^{j+1} is the update/new weed position at j^{th} iteration, V_{best} is the best weed found in the whole population. δ_i is a standard Cauchy

$$\text{random variable and } m = \Delta V \times \text{sign}\left(\frac{dP_{pv}^{max}}{dV_{mpp}}\right) \quad (8)$$

Here, the value of step change is considered as 0.05V and maximum seeds is 7.

C) **Boost converter**

Fig. 1 depicts the circuit with a controller that will be used for the boost converter for MPPT of PV system. The control signal (i.e., duty cycle (D)) contains pulses with a constant width in a steady state. The switch (S_d) is ON during t_{on} and OFF during t_{off} . The voltage across the inductor (V_L) is equal to the input voltage, V_{pv} , during t_{on} . The inductor current, I_L is proportional to the integral of V_L . In this paper boost converter is a modelled form [37]. Reference DC-voltage (input voltage) of the boost converter is obtained from integration of MIWO with P&O algorithm. This signal is compared with actual input voltage and error is given to proportional plus integral (PI)-controller. The PI-controller can generate duty cycle for S_d . In this paper, integral-time-square-error (ITSE) [33] method is used for tuning the gains of PI-controller. The boost converter controller is

called as a DC-link voltage controller as shown in Fig. 1. The flowchart of the proposed system is shown in Fig. 4.

4. SMALL-SIGNAL ANALYSIS

Non-linear model of the proposed system is obtained by nonlinear equations of the system blocks and corresponding non-linear block diagram of the proposed system (Fig. 1) is shown in Fig. 14. The system has non-linear relations, hence, to investigate the small-signal analysis, one must convert the system to a linear system. The linearization of the nonlinear model of Fig. 14 is carried out using the small-signal method.

The PV system linearized equation is obtained by (1) & (2) with the small-signal method. A linear time-invariant model for the inductor current to the duty cycle of the boost converter is taken from [39]. The transfer function of inductor current to the duty cycle of the boost converter is followed by (10).

$$\frac{I_L(s)}{D(s)} = \frac{a_1(s + a_2)}{s^2 + a_3s + a_4} \quad (10)$$

where, $a_1 = \frac{V_{pv}}{DL}$, $D' = 1 - D$, $a_2 = \frac{1}{C(R_L + R_c)} \left[1 + \frac{R_L D'}{R_L D' + R_c} \right]$, $a_3 = \frac{L + R_L R_c C_d D'}{(R_L + R_c) LC_d}$ and

$$a_4 = \frac{R_L D' (R_L D' + R_c)}{LC_d (R_L + R_c)^2} \quad (11)$$

The detailed linear model of the proposed system is shown in Fig. 14. However, linear model of MPPT is neglected and it is considered as one of the input signals to the DC-link voltage controller due to its non-linear characteristics (i.e., it is having a sign function). The value of gains in the voltage controller is $K_p = 0.03$ and $K_i = 5.08$.

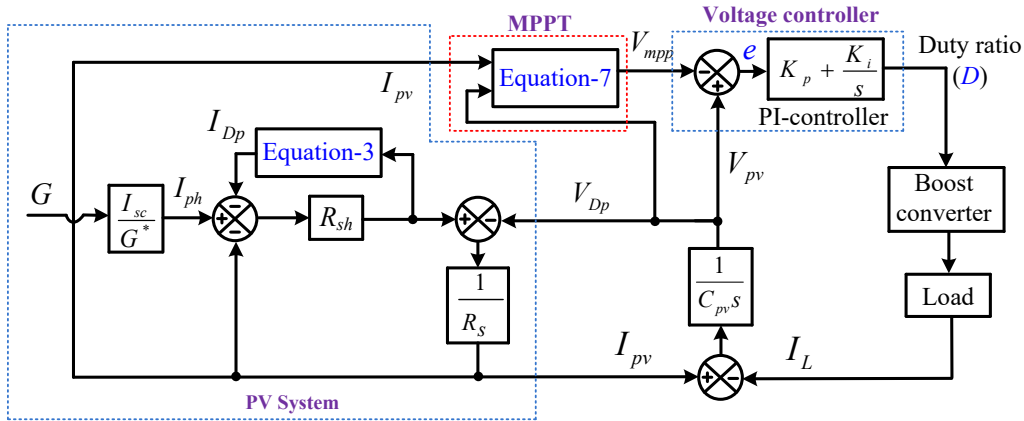


Figure 14. Non-linear model

decreases at $t=3$ s, and the 20% irradiance increases at $t=3.3$ s. The corresponding responses of ΔP_{pv} with an actual system (Fig. 1) and linearized system (i.e., (13)) with load resistances are shown in Fig. 16. It shows that the responses are precisely overlapping, and the response is better in the case of low load resistance, as shown in Fig. 17(c). However, Fig. 16(a) depicts that the system response is slightly different from the linearized system. The load resistance can be adjusted by integrating energy storage such as a battery to system [41]. For better response, the battery can be connected at DC-bus through power electronics devices [42]. Hence, the DC-bus voltage can be regulated by maintaining at a constant load current. The similar responses can be obtained from (15) for change in ΔV_{mpp} .

As is well known, the loop robustness of a feedback system can characterize by gain margin (GM) and phase margin (PM). For a good design, one must have gain margin >6 dB and phase margin $> 30^\circ$ [40]. For robustness study of the system of Fig. 15, loop transfer function is obtained as:

$$L_e = \frac{-d(f_1s^2 + f_2s + f_3)}{g_1s^4 + g_2s^3 + g_3s^2 + g_4s} \quad (16)$$

where, $g_1 = C_{pv}(1 + b_1b_2)$, $g_2 = C_{pv}a_3(1 + b_1b_2) + b_2$, $g_3 = a_4C_{pv}(1 + b_1b_2) + a_3b_2$ and $g_4 = a_4b_2$

The bode plots (indicating gain margin, phase margin, and gain crossover frequency) for the above loop transfer function (i.e., (16)) is presented in Fig. 17 for $R_L=100\Omega$. From Fig. 17, it can be concluded that the system is well robust.

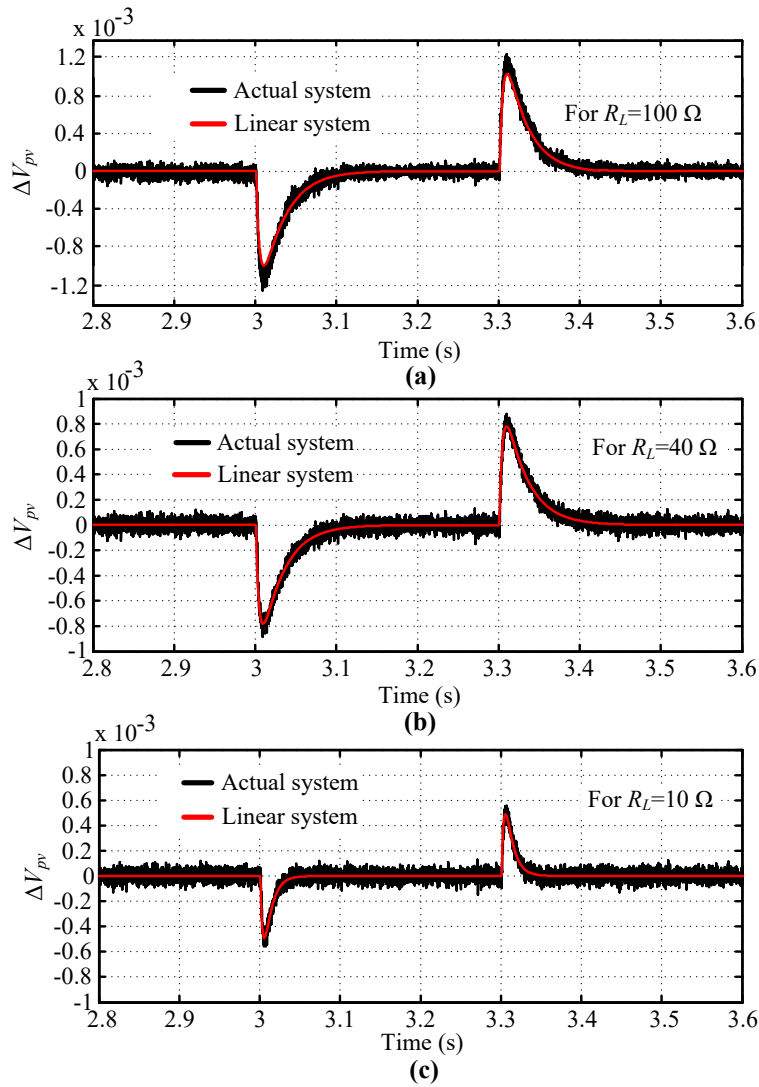


Fig. 16: PV voltage responses of actual and linear system (a). $R_L=100\Omega$, (b). $R_L=40 \Omega$ and (c). $R_L=10\Omega$ load

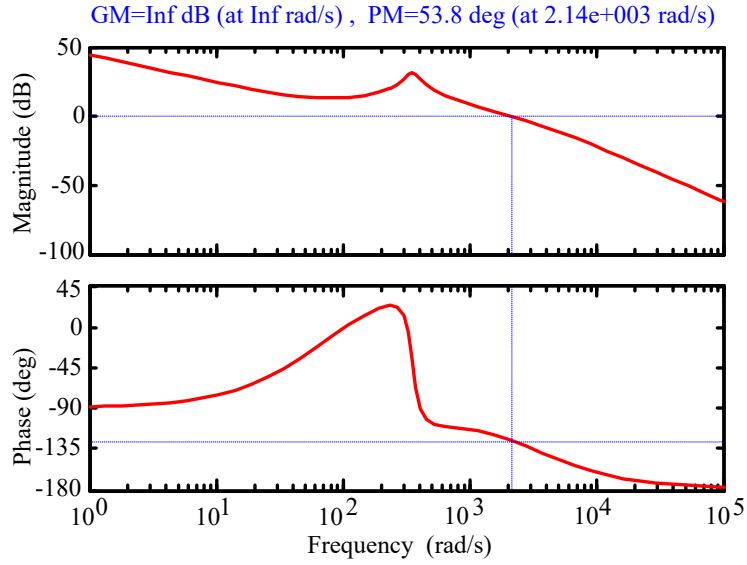


Figure 18. The bode plot for $R_L=40 \Omega$

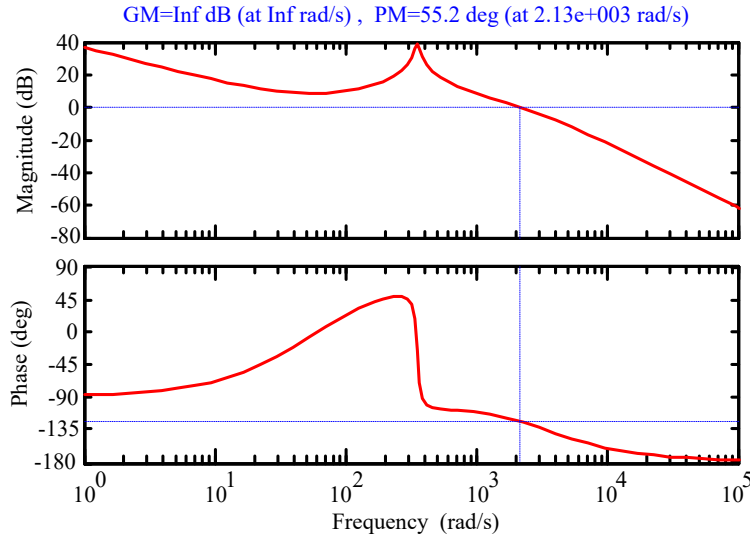


Figure 19. The bode plot for $R_L=100\Omega$

5. SIMULATION RESULTS AND DISCUSSION

4.1. Case-1: MPPT under the change in irradiance

Simulation results are carried out with MATLAB/Simulink. The detailed parameters of PV system are mentioned in Appendix. The simulation results are discussed by considering the following case studies.

Consider that irradiance changes from $1000\text{W}/\text{m}^2$ to $800\text{W}/\text{m}^2$ at the time(t)=1s. As

shown in Fig. 5(a). After a change in irradiance, proposed MPPT algorithm tracked properly V_{mpp} to get maximum power. The boost converter controller operates at V_{mpp} , hence, the system is operating at possible maximum power point. The corresponding V_{mpp} which is generated by the proposed MPPT algorithm as shown in Fig. 5(b). However, decreasing in irradiance can decrease the DC-link voltage in the transient period (see Fig. 5(c)). Hence, MPPT algorithm will increase the reference voltage momentarily which is shown in Fig. 5(b) after $t=1s$. After DC-link starts to increase, MPPT algorithm tries to reduce the reference voltage by voltage steps as follows the Eqn. (8). This reference voltage is input to DC-link controller and boost converter controller regulates the V_{PV} at V_{mpp} as shown in Fig. 5(c). The corresponding power is depicted in Fig. 5 (d). From Fig. 5 (d), it can be concluded that power generated by PV is following its reference signal. The comparative analysis of V_{mpp} voltage during the change in irradiance as given in Table-2 . However, the PV voltage deviation and efficiency during this period is given in Table-3. Table-2, depicts that the proposed algorithm has less deviation of voltage sags and swells as compared to other algorithm. The proposed algorithm has less settling time as compared to GWO-FLC and MBOA method. However, the proposed algorithm has high PV efficiency as well as less voltage deviation as compared to GWO-FLC and MBOA method as given in Table-3.

Table 2: Comparative dynamic V_{mpp} voltage performance

Performance indexes Fig. 5(b)	MPPT [28]	MPPT [27]	Proposed algorithm
Maximum deviation (V_p)	1.5	2	0.5
Minimum deviation (V_d)	3	4	2
Settling time (t_s)	0.15	0.1	0.06

Table 3: Comparative voltage deviation and efficiency (η_{MPPT})

Performance indexes	MPPT [28]	MPPT [27]	Proposed algorithm
Voltage deviation (Fig. 5(c))	3%	4.12%	2.05%
PV efficiency (Fig. 5(d))	99.98%	99.978%	99.997%

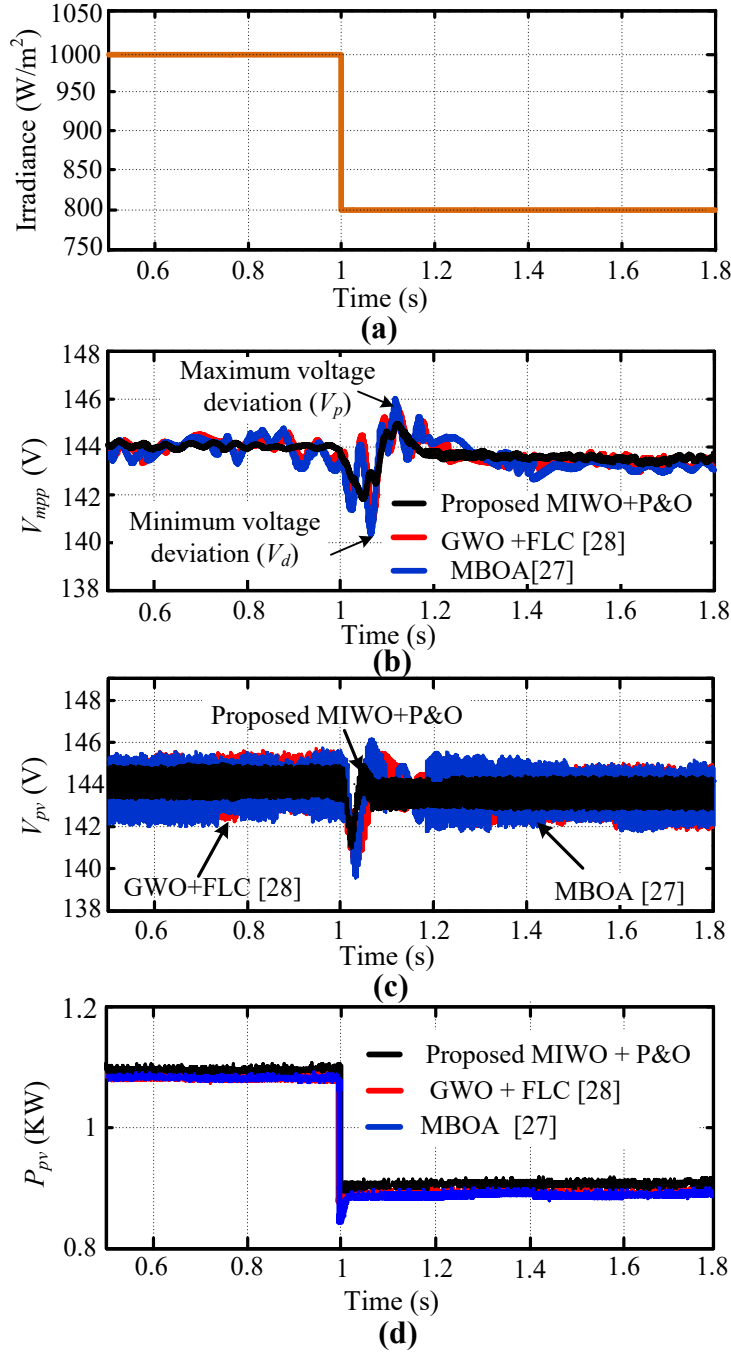


Figure 5: (a). Variation in insolation, (b). Nominal V_{mpp} voltage, (c). V_{pv} , (d). PV power

4.2. Case-2: MPPT under the partial shading

Generally, PV array cannot receive uniform irradiance, under this situation; partial shading effect creates many local maximum power points. The proposed MIWO based MPPT algorithm achieves the proper V_{mpp} corresponding to the global maximum point.

Hence, the system can operate at maximum power point under partial shading condition. The conventional P&O algorithm can extract voltage corresponding to a first local minimum (which is near to present voltage point). Hence, integration of P&O with MIWO algorithm can work better and extract more power from the PV system in all the possible cases.

Now considered partial shading occurs at $t=2.5s$. Corresponding PV power is shown in Fig. 6. From Fig.6, it can be concluded that, power generated from PV system is following possible maximum power from the PV system under partial shading condition. Hence, proposed controller can be able to extract maximum power from a PV system. In order to provide the accuracy of the proposed algorithm, the actual extraction of PV output power during PSC is shown in Fig. 7. In this case the solar irradiance of each PV module is different. From Fig 7, the tracking efficiency (η_{MPPT}) contributes higher tracking efficiency as compared to GWO-FLC [28] and MBOA [27]. The exact value of the η_{MPPT} is provided in Table-4. From the above results, it can be concluded that the suggested MIWO-P&O technique has a good tracking competency with improved PV voltage control capability (i.e., lower peaks/dips) as compared to the GWO-FLC [28] and MBOA [27] based hybrid MPPT techniques.

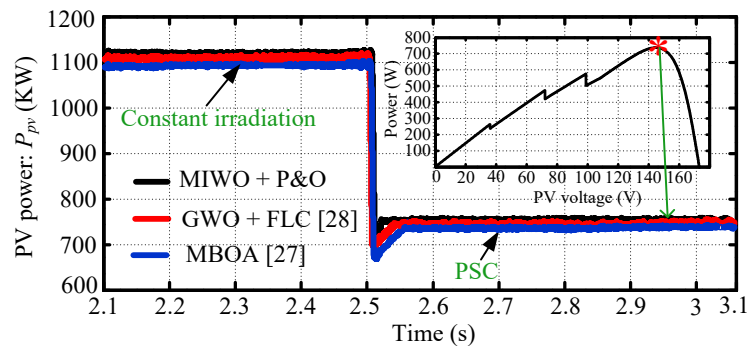


Figure 7. PV power under partial shading

Table 4: Comparative efficiency (η_{MPPT})

Performance index	MPPT [27]	MPPT [28]	Proposed algorithm
PV efficiency	99.75%	99.85%	99.97%

4.3. Case-3: Performance evaluation for the presence of uncertainty

In this case, the effectiveness/robustness of the proposed controller is tested in the presence of uncertainty in the boost converter. The proposed system uses closed loop

control algorithm. If this system has may kind of parameter variation or model uncertainty like inductance, capacitance etc. the output still convergence to the desired level. For analysis, the uncertainty is added in the capacitor of +10% variation as shown in Fig.1. This has been tested in 10% deviation of capacitance value and the corresponding DC-bus voltage is found to be within the 1% of nominal value which is acceptable shown in Fig. 8. Moreover, the frequency response of the system is shown in Fig. 9. From Fig. 9, it can be concluding that it does not affect the uncertainty using the proposed control algorithm.

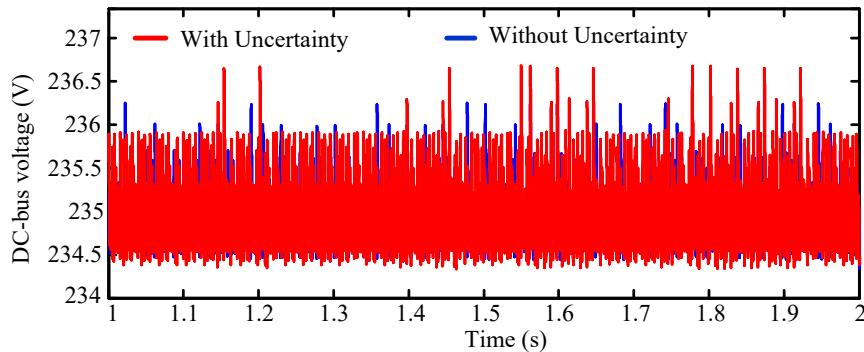


Figure 8. DC-bus voltage on uncertainty condition

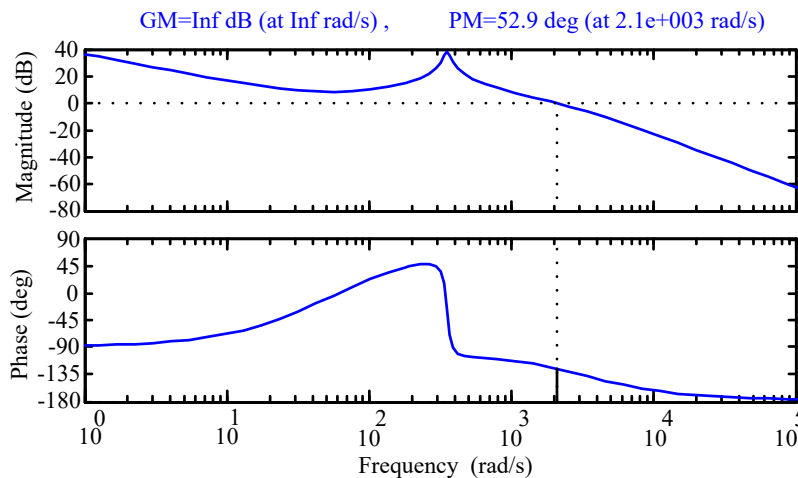


Figure 9. System frequency response during uncertainty

6. EXPERIMENTAL RESULTS AND DISCUSSIONS

Hardware results are carried out with 1.12 kW PV system which is same as MATLAB model. The implementation of the hardware setup is done by using dSPACE real-time control [38]. The proposed controller interfaced with boost converter switch (i.e., S_d) through dSPACE. I_{PV} and V_{PV} are sensed and these signals are given as inputs to dSPACE. The detailed experimental setup is shown in Fig. 10. Partial shading portion is highlighted in Fig. 8. However, light partial shading is also distributed around PV modules. The results

with dSPACE are also shown in Fig. 10. The results obtained from the computer (through dSPACE, i.e., portion 3 in Fig. 10) are converted to MATLAB and provided in following cases studies.

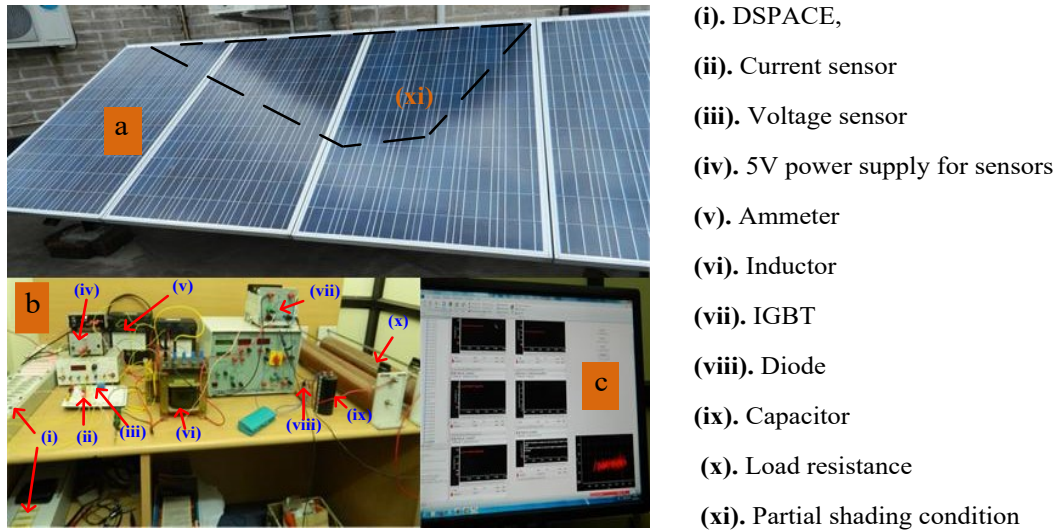


Figure 10: Experimental setup of the studied PV system (a). PV system under partial shading, (b). dSPACE based boost converter control, (c). Result with dSPACE

6.1 Case-1: Under Uniform solar irradiance

In this case, uniform irradiance considered i.e 1000w/m^2 for $t= 0$ to 70s . During this period the corresponding PV power is shown in Fig.11. During this period, the PV power is 1118W using GWO assisted FLC method. However, using MBOA method the PV power is 1116W . The proposed MIWO algorithm gives 1119W . From this Fig 11. it concluded that the controller is extracting maximum available power from a PV system during uniform solar irradiance condition. It is possible because MIWO with P&O algorithm which is helpful to track a proper V_{mpp} .

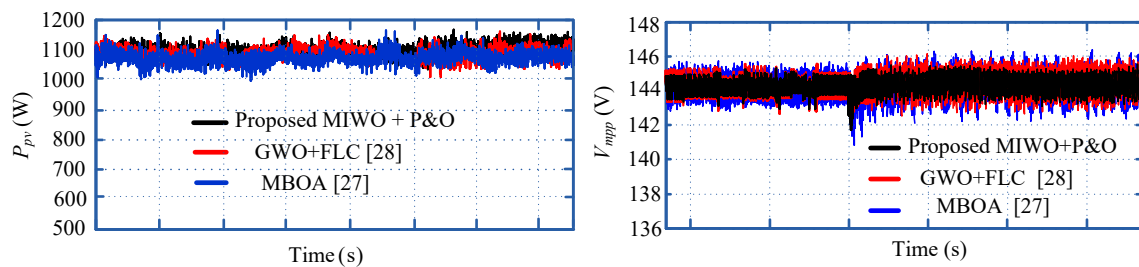


Figure 11: (a). PV power using proposed algorithm, GWO+FLC and MBOA algorithm, (b). PV voltage during noisy condition

In this case, the robustness of the proposed control strategy is tested in the presence of noise. This noise is inserted into the system when voltage and current are measured. Assume that an expected noise of 50dB signal to noise ratio is inserted in PV voltage as shown in Fig. 1. For the analysis, the noise was added at $t=30s$ on the PV voltage as shown in Fig. 11(b). From, the Fig. 11(b), it is observed that the voltage dynamics of the photovoltaic voltage in the presence of noise is improved significantly using the proposed controller.

In this case, the effectiveness/robustness of the proposed controller is tested in the presence of noise in the PV system. This noise is inserted into the system when the voltage and current are measured. Assume an expected noise of 40dB signal to noise ratio (SNR) is inserted in the PV voltage as shown in Fig. I. For analysis, the noise was added at the time (t)= $30s$ on the PV voltage as shown in Fig. 11(b). The SNR is usually expressed in terms of the logarithmic decibel scale as follows:

$$SNR(dB) = 10 \log_{10} \left(\frac{P_{signal}}{P_{noise}} \right) = 20 \log_{10} \left(\frac{V_{signal}}{V_{noise}} \right) \quad (9)$$

where, P_{signal} and P_{noise} represent the average received signal power and noise power, respectively. V_{signal} and V_{noise} are the corresponding signal voltage and noise voltage, respectively.

In this case study, the solar insolation for each PV string is taken as $1000W/m^2$. From Fig. 11(a), it can be seen that the proposed controller significantly improves the dynamics of the DC-link voltage PV in the presence of noise in photovoltaic power systems.

5.2 Case-2: Under partial shading PSC-1

In this case, non-uniform irradiance considered for $t=2s$ to $18s$. During this period the corresponding current, voltage and PV power is shown in Fig.12. During PSC-1 as per Fig. 3, the PV power is $702.9W$ using GWO assisted FLC method. However, using MBOA method the PV power is $705.2W$. The proposed MIWO algorithm gives $706.82W$. From this Fig 11. it concluded that the controller is extracting maximum available power from a PV system during partial shading condition. The corresponding voltage becomes approximately $144V, 144.1V$ and $144.3V$ respectively, in steady-state condition. Fig.11 depicts that the proposed algorithm extracts more PV power than other algorithms. It is possible because MIWO with P&O algorithm which is helpful to track a proper V_{mpp} . The corresponding MPPT tracking efficiency is $99.81\%, 99.89\%, 99.97\%$: respectively, using, MBOA, GWO assisted FLC algorithm and Proposed MIWO assisted P&O algorithm.

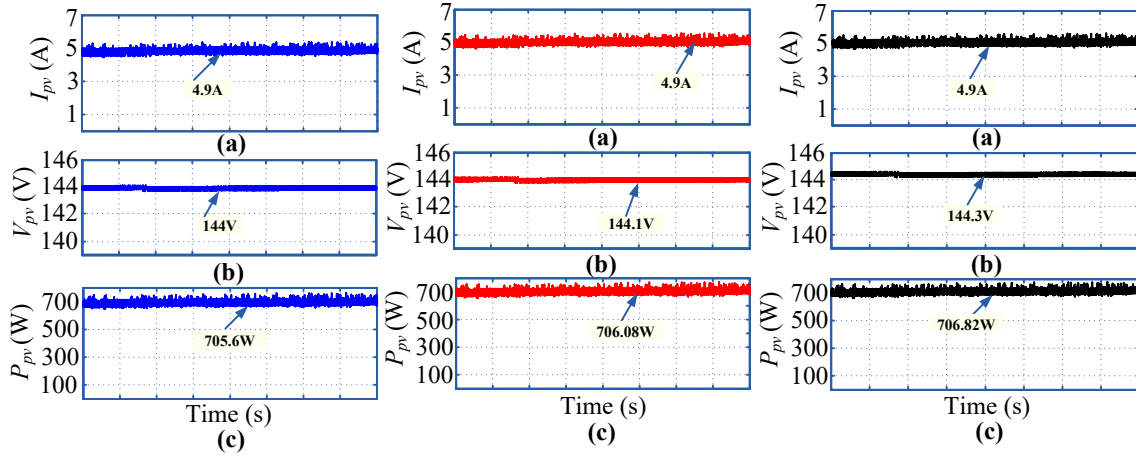


Fig. 12: PSC-1 (a) PV current, (b) PV voltage, (c) PV power using MBOA method, GWO+FLC method and MIWO+P&O method, respectively.

5.3 Case-3: Under partial shading PSC-2

In this case, non-uniform irradiance considered for $t=2s$ to $18s$. During this period the corresponding current, voltage and PV power is shown in Fig.13. During PSC-2 as per Fig. 3, the PV power is 551.95W using MBOA method. However, using GWO assisted FLC method the PV power is 555.05W. The proposed MIWO algorithm gives 556.42W. From this Fig 12. it concluded that the controller is extracting maximum available power from a PV system during partial shading condition. The corresponding voltage becomes approximately 143.9V, 144V and 144.2V respectively, in steady-state condition. Fig.12 depicts that the proposed algorithm extracts more PV power than other algorithms. It is possible because MIWO with P&O algorithm which is helpful to track a proper V_{mpp} . The corresponding MPPT tracking efficiency is 99.75%, 99.81%, 99.968% respectively, using, MBOA, GWO assisted FLC algorithm and Proposed MIWO assisted P&O algorithm.

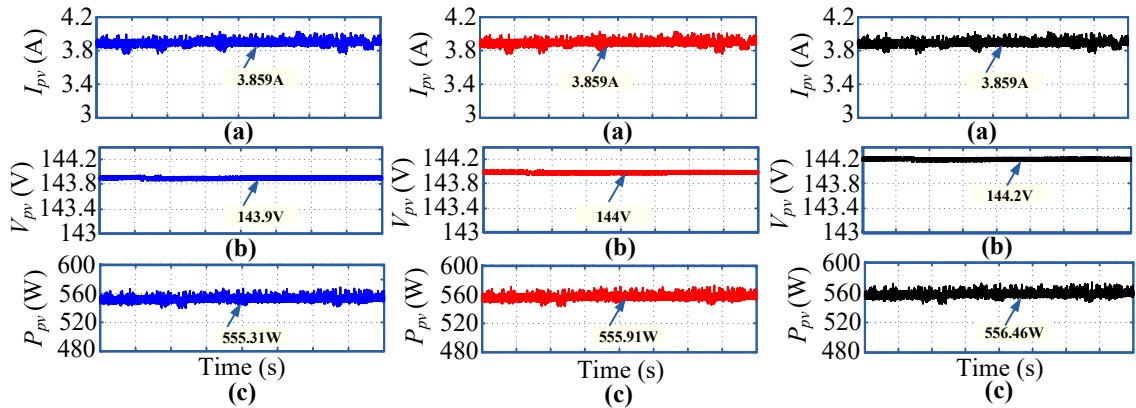


Fig. 12: PSC-2 (a) PV current, (b) PV voltage, (c) PV power using, MBOA method, GWO+FLC method and MIWO+P&O method, respectively.

5.4 Case-4: Load variation under partial shading condition

The efficacy of the proposed algorithm can be tested on the variation load. Initially, it is tested on the load of 10Ω , after that another load is connected of 10Ω to the system. The details response of PV power, PV voltage and current during load variation is shown in Fig. 13. From Fig. 13(a), it is observed that in load variation PV power can track easily to the MPPT. However, the voltage is decreased when the load varied from 10Ω to 20Ω . At the same time current increases to some extent as shown in Fig. 13(c) and 13(b) respectively. Hence, the proposed algorithm is robust for the load variation.

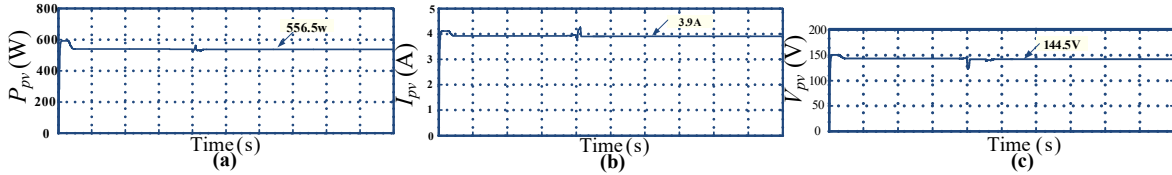


Fig. 13: PSC-2 (a) PV current, (b) PV voltage, (c) PV power using MIWO+P&O method.

7. CONCLUSION

MIWO integrated with P&O algorithm based stand-alone PV based power generation system is presented in this paper. MIWO is integrated with a P&O algorithm for an effective operation of MPPT system under partially shaded PV system. Boost converter is considered for MPPT converter to extract the maximum power from PV. Using boost converter control, the power balance between PV and load is achieved by varying duty cycles. The PV system is operating at maximum power level in both normal as well as partial shading condition by regulating (V_{pv}) corresponding to V_{mpp} (generated by MPPT algorithm) with the boost converter controller. In this paper, the battery is not considered; however, the response of the system can increase by adding a battery to the system. Small-signal analysis is also done to show the strength of the theory. The controller is tested in hardware and presented hardware results with the help of dSPACE. The different cases are discussed based upon changes in solar irradiance and partial shading condition. Loop robustness is presented with the help of a Bode plot of the loop transfer function. Through the MATLAB based simulation and dSPACE based hardware (real-time) results, it is concluded that the performance of the controllers is satisfactory under conditions of changes in irradiance as well as under partial shading.

8. LIST OF SYMBOLS AND ABBREVIATIONS

8.1. Nomenclature

I_{ph} Current of PV cell (A)

I_o	Load current (A)
I_{rs}	Diode reverse saturation current (A)
R_s	Series resistance of the PV module (Ω)
R_{sh}	Shunt resistance of the PV module (Ω)
V_{pv}	Photovoltaic voltage (V)
T	Array temperature (0K)
I_{rr}	Reverse saturation current (A)
T_r	Cell reference temperature (A)
I_{sc}	Short circuit current (A)
G	Solar irradiance (W/m^2)
q	Electron charge (C)
V_{oc}	Open circuit voltage (V)
K	Iteration
V_{mpp}	Nominal voltage (V)
ΔV	Step voltage
σ_{gen}	Standard deviation
σ_{max}	Maximum standard deviation
σ_{min}	Minimum standard deviation
mi	Nonlinear modulation index
Gen_{max}	Maximum generation
W_{max}	Maximum seeds are generated
δ_i	Cauchy random variable

8.2. Abbreviations

PV	Photovoltaic
MIWO	Modified Invasive Weed Optimization
P&O	Perturb & Observe
MPP	Maximum power point
MPPT	Maximum power point tracking
PSC	Partial shading condition
RES	Renewable energy sources
GMPP	Global maximum power point

PWM	Pulse width modulation
PI	Proportional plus integral

9. REFERENCES

1. M. Liserre, T. Sauter, and J. Y. Hung, "Renewable Energy Systems, Integrating Renewable Energy Sources into the Smart Power Grid through Industrial Electronics," *IEEE Industrial Electronics Magazine*, vol. 4, no. 1, pp. 18-37, March 2010.
2. G. Li, Y. Jin, M. W. Akram, X. Chen, and J. Ji, "Application of Bio-inspired Algorithms in Maximum Power Point Tracking for PV Systems under Partial Shading Conditions—A Review," *Renewable and Sustainable Energy Reviews*, vol. 81, no. 1, pp. 840-873, January 2018.
3. X. Li, *et al.*, "Comprehensive Studies on Operational Principles for Maximum Power Point Tracking in Photovoltaic Systems," *IEEE Access*, vol. 7, pp. 121407-121420, September 2019.
4. J. Ahmed, and Z. Salam, "A Modified P&O Maximum Power Point Tracking Method with Reduced Steady State Oscillation and Improved Tracking Efficiency," *IEEE Trans. on Sustainable Energy*, vol. 7, no. 4, pp. 1506-1515, October 2016.
5. F. Belhachat, and C. Larbes, "A Review of Global Maximum Power Point Tracking Techniques of Photovoltaic System under Partial Shading Conditions," *Renewable and Sustainable Energy Reviews*, vol. 92, pp. 513-553, September 2018.
6. A. Mohapatra, B. Nayak, P. Das, and K. B. Mohanty, "A Review on MPPT Techniques of PV System under Partial Shading Condition," *Renewable and Sustainable Energy Reviews*, vol. 80, pp. 854-867, December 2017.
7. Karami, N., Moubayed, N., and Outbib, R, "General review and classification of different MPPT Techniques," *Renewable and Sustainable Energy Reviews*, Vol.68, pp. 1–18, February 2017.
8. S. Motahhir, A. El Hammoumi, and A. El Ghziza, "The most used MPPT algorithms: Review and the suitable low-cost embedded board for each algorithm," *Journal of Cleaner Production*, vol. 246, no. 1, pp. 1–17, February 2020.
9. K. S. Tey, and S. Mekhilef, "Modified Incremental Conductance Algorithm for Photovoltaic System Under Partial Shading Conditions and Load Variation", *IEEE Trans. on Industrial Electronics*, vol. 61, no. 10, pp. 5384–5392, May 2014.
10. M. Seyedmahmoudian, *et al.*, "State of the art artificial intelligence-based MPPT techniques for mitigating partial shading effects on PV systems – A review," *Renewable and Sustainable Energy Reviews*, vol. 64, pp. 435–455, June 2016.
11. B. N. Alajmi, K. H. Ahmed, S. J. Finney, and B. W. Williams, "Fuzzy-logic-control approach of a modified hill-climbing method for maximum power point in microgrid standalone photovoltaic system," *IEEE Trans. on Power Electronics*, vol. 26, no. 4, pp. 1022–1030, April 2011.

12. C. F. Juang, C. W. Hung, and C. H. Hsu, "Rule-Based Cooperative Continuous Ant Colony Optimization to Improve the Accuracy of Fuzzy System Design," *IEEE Trans. on Fuzzy Systems*, vol. 22, no. 4, pp. 723–735, August 2014.
13. L. Bouselham, M. Hajji, B. Hajji, and H. Bouali, "A new MPPT-based ANN for photovoltaic system under partial shading conditions," *Energy Procedia*, vol. 111, pp. 924–33, March 2017.
14. S. Farajdadian and S. M. H. Hosseini, "Optimization of fuzzy-based MPPT controller via Metaheuristic techniques for stand-alone PV systems," *Int. J. Hydrogen Energy*, vol. 44, no. 47, pp. 25457–25472, Oct. 2019.
15. M. N. Ali, K. Mahmoud, M. Lehtonen and M. M. F. Darwish, "An Efficient Fuzzy-Logic Based Variable-Step Incremental Conductance MPPT Method for Grid-Connected PV Systems," *IEEE Access*, vol. 9, pp. 26420-26430, 2021.
16. A. Harrag and S. Messalti, "IC-based variable step size neuro-fuzzy MPPT improving PV system performances," *Energy Procedia*, vol. 157, pp. 362–374, January 2019.
17. A. Messai, A. Mellit, A. Guessoum, and S. A. Kalogirou, "Maximum Power Point Tracking using GA optimized FLC and its FPGA Implementation," *Solar energy*, vol. 85, no. 2, pp. 265-277, 2011.
18. A. A. Kulaksiz, R. Akkaya, "A Genetic Algorithm Optimized ANN Based MPPT Algorithm for a Stand-Alone PV System with Induction Motor Drive," *Solar Energy*, Vol. 86, no. 9, pp. 2366-2375, September 2012.
19. A. K. Podder; N. K. Roy; and H. Roy Pota, "MPPT methods for solar PV systems: a critical review based on tracking nature," *IET Renewable Power Generation*, vol. 13, no. 10, pp. 1615-1632, July 2019.
20. K. Ishaque, and Z. Salam, "A Deterministic Particle Swarm Optimization Maximum Power Point Tracker for Photovoltaic System under Partial Shading Condition," *IEEE Trans. On Industrial Electronics*, vol. 60, no. 8, pp. 3195–3207, August 2013.
21. S. Titri, *et al.*, "A New MPPT Controller Based on the Ant Colony Optimization Algorithm for Photovoltaic Systems under Partial Shading Conditions," *Applied Soft Computing*, vol. 58, pp. 465–79, September 2017.
22. Y. P. Huang, M. Y. Huang; and C. E. Ye, "A Fusion Firefly Algorithm with Simplified Propagation for Photovoltaic MPPT under Partial Shading Conditions," *IEEE Trans. on Sustainable Energy*, vol. 11, no. 4, pp. 2641-2652, October 2020.
23. X. Ge, F. W. Ahmed, A. Rezvani, N. Aljojo, S. Samad, and L. K. Foong, "Implementation of a novel hybrid BAT-fuzzy controller based MPPT for grid-connected PV-battery system," *Control Eng. Pract.*, vol. 98, May 2020, Art. no. 104380
24. S. Lyden, and M. D. E. Haque, "A simulated annealing global maximum power point tracking approach for PV modules under partial shading conditions", *IEEE Trans. on Power Electronics*; vol. 31, no. 6, pp. 4171–4181, June 2016.
25. A. A. Z. Diab, and H. Rezk, "Global MPPT based on flower pollination and differential evolution algorithms to mitigate partial shading in building integrated PV system," *Solar Energy*, vol. 157, pp.171–186, November 2017.
26. C. Huang *et al.*, "A Prediction Model Guided Jaya Algorithm for the PV System Maximum Power Point Tracking," *IEEE Trans. on Sustainable Energy*, vol. 9, no. 1, pp. 45-55, January 2018.

27. I. Shams, D. S. Mekhilef, and K.S. T., "Maximum Power Point Tracking using Modified Butterfly Optimization Algorithm for Partial Shading, Uniform Shading and Fast Varying Load Conditions," *IEEE Trans. on Power Electronics*, vol. 36, no. 5, pp. 5569-5581, May 2021.
28. A. M. Eltamaly, and H. M. H. Farh, "Dynamic Global Maximum Power Point Tracking of the PV Systems under Variant Partial Shading Using Hybrid GWO-FLC", *Solar Energy*, vol. 177, pp. 306–316, August 2019.
29. K. Sundareswaran, V. Kumar, and S. Palani, "Application of a Combined Particle Swarm Optimization and Perturb and Observe Method for MPPT in PV Systems under Partial Shading Conditions," *Renewable Energy*, vol. 75, pp. 308–317, March 2015.
30. N. Kumar, I. Hussain, B. Singh, and B. K. Panigrahi, "Rapid MPPT for Uniformly and Partial Shaded PV System by Using Jaya DE algorithm in Highly Fluctuating Atmospheric Conditions," *IEEE Trans. on Industrial Information*, vol. 13, no. 5, pp. 2406–2416, October 2017.
31. M. Seyedmahmoudian, R. Rahmani, *et al.*, "Simulation and Hardware Implementation of New Maximum Power Point Tracking Technique for Partially Shaded PV System Using Hybrid DEPSO Method," *IEEE Trans. on Sustainable Energy*, vol.6, no.3, pp.850–862, February 2015.
32. M. Misaghi, and M. Yaghoobi, "Improved Invasive Weed Optimization Algorithm (IWO) based on Chaos Theory for Optimal Design of PID Controller," *Journal of Computational Design and Engineering*, vol. 6, no. 3, pp. 284-295, July 2019.
33. M. K. Senapati, C. Pradhan, S. R. Samantaray, and P. K. Nayak, "Improved power management control strategy for renewable energy-based DC micro-grid with energy storage integration," *IET Generation, Transmission & Distribution*, vol. 13, no. 6, pp. 838-849, May 2019.
34. L. F. L. Villa, *et al.*, "A Power Electronics Equalizer Application for Partially Shaded Photovoltaic Modules," *IEEE Trans. on Industrial Electronics*, vol. 60, no. 3, pp. 1179-1190, March 2013.
35. C. N. Bhende, and S. G. Malla, "Novel Control of Photovoltaic based Water Pumping System without Energy Storage," *International Journal of Emerging Electric Power Systems*, vol. 13, no. 5, November 2012.
36. S. Yuantao, and Z. Qing, "Based on the Cauchy Distribution Reproduce Mode Improved IWO Algorithm Research and Application," *2nd International Conference on Information Science and Engineering (ICISE)*, Hangzhou, China, pp. 1057-1060, 4-6 December 2010.
37. Y. Li, *et al.*, "Current Mode Control for Boost Converters with Constant Power Loads," *IEEE Trans. on Circuits and Systems-I: Regular papers*, vol. 59, no. 1, pp. 198-206, January 2012.
38. A. M. Noman, K. E. Addoweesh, and H. M. Mashaly, "DSPACE Real-Time Implementation of MPPT-Based FLC Method," *International Journal of Photo energy*, vol. 2013, Article ID 549273, 11 pages, 2013.
39. B. Johansson, "Improved Models for DC-DC Converters", Licentiate Thesis, Department of Industrial Electrical Engineering and Automation, Lund University, Lund, 2003.
40. R. C. Dorf, and R. H. Bishop, "Modern Control Systems," Pearson Education, Inc, 2008.
41. H. Beltran, *et al.*, "Evaluation of Storage Energy Requirements for Constant Production in PV Power Plants," *IEEE Trans. on Industrial Electronics*, vol. 60, no. 3, pp. 1225-1234, March 2013.

42. B. K. Bose, "Global Energy Scenario and Impact of Power Electronics in 21st Century," IEEE Trans. on Industrial Electronics, vol. 60, no. 7, pp. 2638-2651, July 2013.
43. <http://www.4-dgroup.com/4d/PDF/Tata%20300.pdf>

APPENDIX

Parameters of PV module

<i>For both simulation and experiment [43]</i>	
Module Type	TP280
Maximum power (P_{pvmax})	280 W
Open circuit voltage (V_{oc})	44 V
Short circuit current (I_{sc})	8.28 A
Voltage at P_{pvmax} (V_{mpp})	36.2 V
Current at P_{pvmax} (I_{mpp})	7.73 A
Series resistance per cell (R_s)	0.0040 Ω
Parallel resistance per cell (R_p)	4.106 Ω
Module efficiency	14.1
Power tolerance	[-0 & +5]
Number of modules connected in series (n_s)	4

Parameters of boost converter

<i>For both simulation and experiment</i>	
Capacitance (C & C_{pv})	1000 μ F
Inductor (L)	1.3mH
Resistance (R_C)	0.15 Ω
Duty cycle (D)	0.6

Parameters used in small-signal model

Parameters	$R_L=10 \Omega$	$R_L=40 \Omega$	$R_L=100 \Omega$
a_1	2.7846×10^5	2.7846×10^5	2.7846×10^5
a_2	193.4833	49.5819	19.484723
a_3	143.9939	70.8880	28.45723
a_4	1.2395×10^5	1.233×10^5	1.2302×10^5
a_5	8.6032×10^{-5}	8.6032×10^{-5}	8.6032×10^{-5}
b_1	0.003	0.003	0.003
b_2	3.4316	3.4316	3.4316
b_3	0.0010	0.0010	0.0010
b_4	3.5771	3.5033	3.477
b_5	9.0600×10^3	8.8085×10^3	8.47524×10^3
b_6	34.877×10^5	22.709×10^5	14.729×10^5
b_7	2765.40×10^5	708.670×10^5	282.1836×10^5
d	2.8135×10^5	2.8135×10^5	2.8135×10^5
f_1	0.03	0.03	0.03
f_2	10.8845	6.5675	3.9563
f_3	982.8951	251.8759	100.727
g_1	0.0010	0.00101	0.0010102
g_2	3.5771	3.5033	3.47
g_3	619.3674	367.8467	221.9402
g_4	4.2534×10^5	4.2313×10^5	4.2215×10^5